CASE REPORT   **Open Access**

Navigating the diagnostic gray zone: a challenging case of pancreatic high-grade neuroendocrine neoplasm

Brooke Mullen[1†], Albert L. Sy[1,2†], Priscila Dias Goncalves[1,2] and M. Lisa Zhang[1,2*]

Abstract

Background Grade 3 neuroendocrine tumor (G3 PanNET) and poorly differentiated neuroendocrine carcinoma (PanNEC) of the pancreas are considered distinct entities from a biological and prognostic perspective but may have overlapping features complicating a definitive diagnosis.

Case Presentation A 52-year-old female presented with a pancreatic body mass and liver lesions. Initial biopsies showed variable lower- and higher-grade morphologies and modestly elevated Ki67 proliferation index up to 30%, leading to a diagnosis of G3 PanNET. The patient underwent everolimus treatment followed by surgical resection, revealing a complex tumor with features of both G3 PanNET and PanNEC, including admixed well- and poorly differentiated morphologies, modestly elevated hotspot Ki67 of 28%, retained ATRX/DAXX expression, and loss of RB expression. The final diagnosis rendered was "high-grade neuroendocrine neoplasm" with discussion of both entities in the differential. Post-operatively, the patient remains alive with stable metastases.

Conclusions This case highlights the diagnostic complexities of distinguishing G3 PanNET and PanNEC even with the support of ancillary immunohistochemical and molecular studies. In addition, such cases raise the possibility that G3 PanNET and PanNEC may lie on a spectrum of disease with potential biological overlap.

Keywords Pancreas, Neuroendocrine tumor, Neuroendocrine carcinoma

Introduction

Pancreatic neuroendocrine neoplasms (PanNENs) account for 2–5% of all pancreatic tumors [1]. Of those, the vast majority are well-differentiated pancreatic neuroendocrine tumors (PanNETs) while < 3% are poorly differentiated pancreatic neuroendocrine carcinomas (PanNECs). PanNETs may either be functional or non-functional, depending on their ability to secrete hormones and elicit symptoms. Given the frequently indolent, slow-growing, and asymptomatic nature of non-functional PanNETs, they are often not detected until advanced stages with symptom onset related to tumor size and metastasis. In contrast, PanNECs are highly aggressive tumors associated with rapid disease progression and poor patient prognosis.

The current World Health Organization (WHO) 5th edition classification of PanNENs includes PanNET grades 1, 2, and 3, and PanNEC (small cell and large cell types); histological grading is based on mitotic count per 2 mm^2 and Ki67 proliferation index [1]. A significant

†Brooke Mullen and Albert L. Sy are co-first authors.

*Correspondence:
M. Lisa Zhang
mlzhang@mgh.harvard.edu
[1]Department of Pathology, Massachusetts General Hospital, 55 Fruit Street, 02114 Boston, MA, USA
[2]Harvard Medical School, Boston, MA, USA

change from the previous WHO 4th edition classification was the introduction of grade 3 (G3) PanNET as a separate entity from PanNEC, both of which are considered high-grade and defined as having > 20 mitoses per 2 mm^2 or a Ki-67 proliferation index of > 20%. Thus, initially, the distinction between G3 PanNET and PanNEC was primarily based on morphologic evaluation of cytohistological atypia, whereby G3 PanNETs maintain an appreciable well-differentiated neuroendocrine morphology while PanNECs appear as poorly differentiated carcinomas with overtly malignant cells but express markers of neuroendocrine differentiation [2, 3].

Accurate histopathological diagnosis is essential to clinical management. Complete surgical resection is typically the first-line treatment option for G3 PanNETs, whereas upfront platinum-based chemotherapy is used in the setting of poorly differentiated PanNECs. However, despite the definitions of these as distinct entities with respect to diagnosis and clinical behavior, an increasing number of cases straddling the boundary between G3 PanNET and PanNEC—that is, exhibiting overlapping/equivocal histopathological features—have been encountered in clinical practice. Even with the assistance of ancillary immunohistochemical markers, there remain challenging cases for which definitive classification remains elusive. Herein, we present a particularly challenging and illustrative case of a high-grade PanNEN and discuss the clinical, histological, immunophenotypic, and molecular findings.

Case presentation

A 52-year-old female with a remote history of opioid abuse, cigarette smoking, alcohol consumption, hepatitis C infection, and acute pancreatitis presented to the emergency department complaining of general malaise, nausea, vomiting, abdominal pain radiating to the back, and unintentional weight loss over the past six months. Laboratory workup found an elevated serum lipase level of 495 U/L (reference range: 13–60 U/L).

A computed tomography (CT) scan of the abdomen and pelvis demonstrated evidence of acute on chronic pancreatitis with dilation of the pancreatic duct, a 2.2 cm lesion in the pancreatic body (FDG-avid on PET/CT scan), and a large cystic lesion in the pancreatic tail, likely representing a pseudocyst secondary to chronic ductal obstruction by the pancreatic body mass (Fig. 1A-B). Follow-up magnetic resonance imaging (MRI) also revealed two FDG-avid lesions in the right liver measuring 1.5 and 1.4 cm, respectively (Fig. 1C-D). Endoscopic ultrasound-guided fine needle aspiration biopsy (EUS-FNAB) of the pancreatic mass and liver lesions were performed for diagnostic purposes.

Histopathology of initial biopsies

Core biopsies of the pancreatic body mass and a liver mass were obtained. The pancreatic mass consisted of solid sheets and nests of epithelioid cells with dense chromatin and variable amounts of cytoplasm in a background of fibrotic stroma (Fig. 2A). Some areas demonstrated increased nuclear pleomorphism and possible nuclear molding (Fig. 2B). Mitoses and apoptotic bodies were identified. Immunohistochemistry showed that the tumor cells were positive for synaptophysin, chromogranin, and INSM1 (Fig. 2C-E). The Ki67 proliferation index was elevated at ~ 30% (Fig. 2F). P53 showed a wild-type expression pattern (patchy weak nuclear expression) while RB showed loss of nuclear expression (Fig. 2G-H). Though the differential diagnosis of a poorly differentiated PanNEC was raised (supported by the increased degree of nuclear atypia and loss of RB), the biopsy was ultimately finalized as a G3 well-differentiated PanNET given the relatively low Ki67 proliferation index and lower grade liver biopsy findings (discussed below).

Core biopsy of one of the liver masses showed nests and cords of epithelioid cells that appeared more well-differentiated than those seen in the pancreatic biopsy with overall uniform nuclei, fine even chromatin, and variable amounts of cytoplasm; focal areas demonstrated increased pleomorphism (Fig. 2I-K). Rare mitoses were identified. Immunohistochemistry showed that the tumor cells were positive for CAM5.2, synaptophysin, chromogranin, and INSM1 (Fig. 2L). ATRX showed intact nuclear expression (Fig. 2M). Ki67 showed a more modestly increased proliferation index of ~ 13% (Fig. 2N). P53 showed a wild-type pattern, but RB showed retained nuclear expression (Fig. 2O-P). SMAD4 also showed retained expression. A diagnosis of metastatic well-differentiated neuroendocrine tumor (grade 2) was rendered.

Histopathology of pancreatic resection specimen

After multidisciplinary discussion, a three-month cycle of everolimus followed by complete surgical resection was decided as the treatment plan. Repeat abdominal imaging after everolimus treatment demonstrated that her pancreatic mass and liver lesions were unchanged. A distal pancreatectomy with splenectomy was performed. Grossly, the main resection specimen revealed a 2.5×2.4×2.1 cm well-circumscribed, solid tan-white mass in the pancreatic body (Fig. 3). The remaining parenchyma was fibrotic with foci of hemorrhage and dilated main duct and side duct branches, up to 1.3 cm and 0.9 cm, respectively. The pancreatic tail to splenic hilum was remarkable for a 7.2×7.1×6.6 cm pseudocyst with wrinkled lining and a fibrotic wall, 0.3 cm in thickness (3.0 cm away from the body mass).

Histologically, the resection specimen showed a high-grade neuroendocrine neoplasm composed of

Mullen *et al. Diagnostic Pathology*   (2024) 19:123

Page 3 of 8
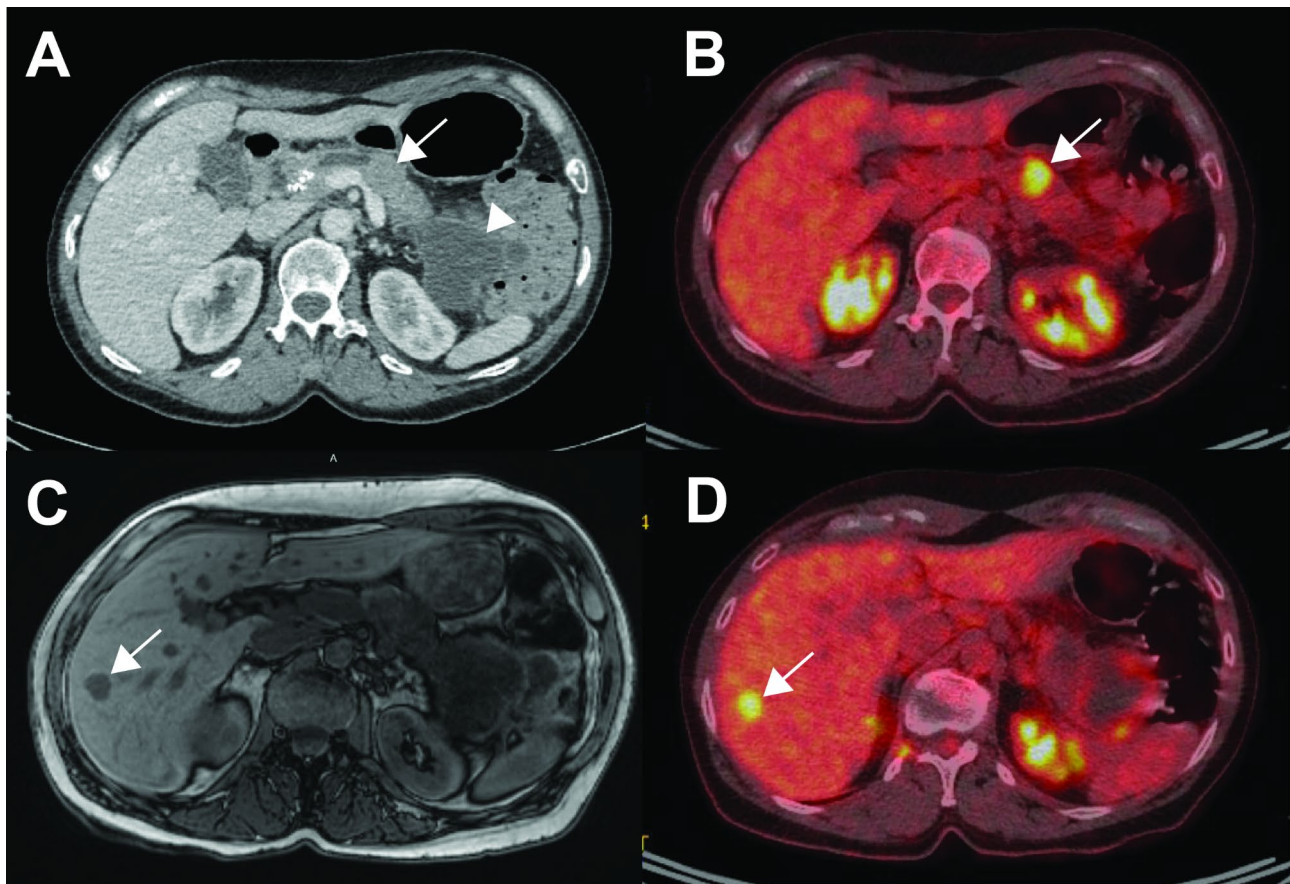
Fig. 1 Pre-operative radiology. **(A)** CT scan and **(B)** corresponding PET/CT demonstrating a 2.2 cm T2 isointense, hypoenhancing mass (arrow) in the pancreatic body with FDG-avidity (arrow) and large cystic lesion in the tail (arrowhead), likely representing a pseudocyst. **(C)** MRI and **(D)** corresponding PET/CT showing one of the hepatic lesions in the right lobe with FDG-avidity (arrows), concerning for metastatic disease.

intermixed areas of morphologically well-differentiated and more poorly differentiated areas (Fig. 4A-F). The well-differentiated areas consisted of well-circumscribed nests of epithelioid cells with monomorphic nuclei, speckled chromatin, and no significant nuclear atypia or pleomorphism (Fig. 4B). The higher-grade areas demonstrated larger nuclei with increased pleomorphism, nuclear membrane irregularities, and variable chromatin quality, with areas of vesicular nuclei (Fig. 4C-D) and other areas with hyperchromatic smudgy chromatin and more scant cytoplasm (Fig. 4E-F). Multiple foci of necrosis were present in the higher-grade/poorly differentiated areas of the tumor. Lymphovascular invasion (Fig. 4G) was also identified, as well as three positive lymph nodes (Fig. 4H). The peak mitotic count was 22 mitoses/2mm^2, and the hotspot Ki67 proliferation index was 28%, though there were multiple areas with a more well-differentiated appearance where Ki67 was <20%. Immunohistochemical stains showed that the tumor cells in all areas were positive for MNF116, synaptophysin, chromogranin, INSM1, ATRX (retained), and DAXX (retained) (Fig. 4). P53 showed patchy wildtype expression, and RB showed

loss of nuclear expression in all areas. P16 expression was heterogeneous, with some nests showing diffuse increased expression while others showed patchy expression, irrespective of morphological appearance (Fig. 4P). The tumor cells were negative for trypsin and BCL10. The well-differentiated morphology and modestly elevated Ki67 (between 20 and 50%) would be more in keeping with a G3 PanNET (which is how the patient was treated prior to resection), but the areas of higher-grade morphology and loss of RB expression would support a poorly differentiated PanNEC. Due to the unusual constellation of morphologic and immunophenotypic findings, a final diagnosis of high-grade PanNEN (with a differential diagnosis of G3 PanNET vs. PanNEC) was rendered.

Histopathology of liver resection specimen
Histologically, resection of the liver metastasis showed a neuroendocrine neoplasm arranged in nests with monomorphic round-to-focally spindled nuclei and coarse chromatin with some prominent nucleoli (Fig. 5A-C). The overall appearance was more homogenous and
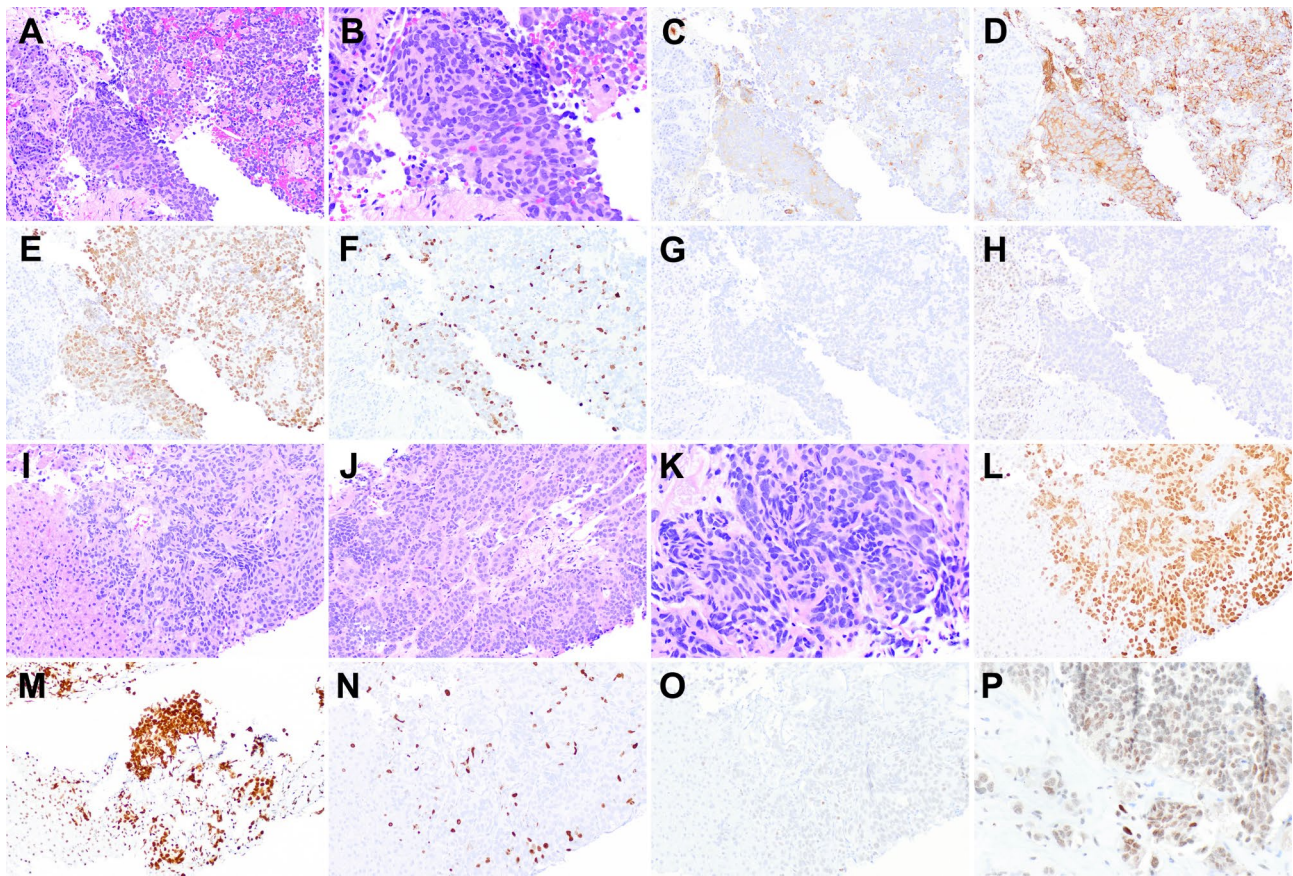
Fig. 2 Histology of core biopsies of the pancreatic mass **(A-H)** and liver mass **(I-P)**. **(A-B)** Pancreatic mass showing sheets of epithelioid cells with dense chromatin and areas of increased nuclear pleomorphism (H&E, 200X and 400X, respectively). Immunohistochemistry for synaptophysin **(C)**, chromogranin **(D)**, INSM1 **(E)**, Ki67 **(F)**, P53 **(G)**, and RB **(H)**, all at 200X. **(I-K)** Liver mass showing a more well-differentiated appearance of nests and cords of overall uniform epithelioid cells with focal pleomorphism (H&E, 200X, 200X, and 400X, respectively). Immunohistochemistry for INSM1 **(L)**, ATRX **(M)**, Ki67 **(N)**, P53 **(O)**, and RB **(P)**, all at 200X except RB (400X).

monomorphic than that seen in the primary tumor. The hotspot Ki67 proliferation index was 8.8% (Fig. 5D), though it was lower in most of the lesion. RB immunohistochemistry showed retained nuclear expression (Fig. 5E), and P16 was largely negative with focal staining (Fig. 5F).

The patient recovered well after surgery. At her 6-month follow-up, the patient remains alive with stable liver, lung, and brain lesions.

Molecular findings

Next-generation sequencing (NGS) was performed on one tumor block containing areas of higher-grade morphology (as shown in Fig. 4C-F). No variants with an established association with this tumor type or other specific tumor types were identified. The following variants (and variant allele frequencies [VAF]) with potential clinical significance were identified: IRS2 p.Q822H (74.0% VAF), IL10 p.K175R (58.5% VAF), TEK p.P568A (37.9% VAF), SMARCA4 p.N248I (29.7% VAF), and NT5C2 p.M15V (20.1% VAF). Tumor mutational burden was low at 7.7 mutations/Mb, and microsatellite status was stable. No copy number variants were detected. Anchored multiplex next-generation fusion assays were negative for reportable fusion transcripts.

Discussion and conclusions

Based on literature over the past decade, our understanding has been that PanNET and PanNEC are distinct entities based on their clinical presentation, response to treatment, disease course, and pathobiology. Notably, 40–50% of PanNETs harbor *ATRX/DAXX* and *MEN1* mutations, which have not been described in PanNECs, while PanNECs may have mutations more typical of high-grade adenocarcinomas such as in *TP53*, *CDKN2A* and *SMAD4*, as well as in *Rb* [4, 5]. Thus, G3 PanNETs are thought to be derived from a neuroendocrine cell lineage and frequently coexist with lower-grade components whereas PanNECs are high-grade carcinomas derived from a glandular/epithelial cell lineage—not arising from progression of PanNET—and can coexist with a component of ductal adenocarcinoma [6].
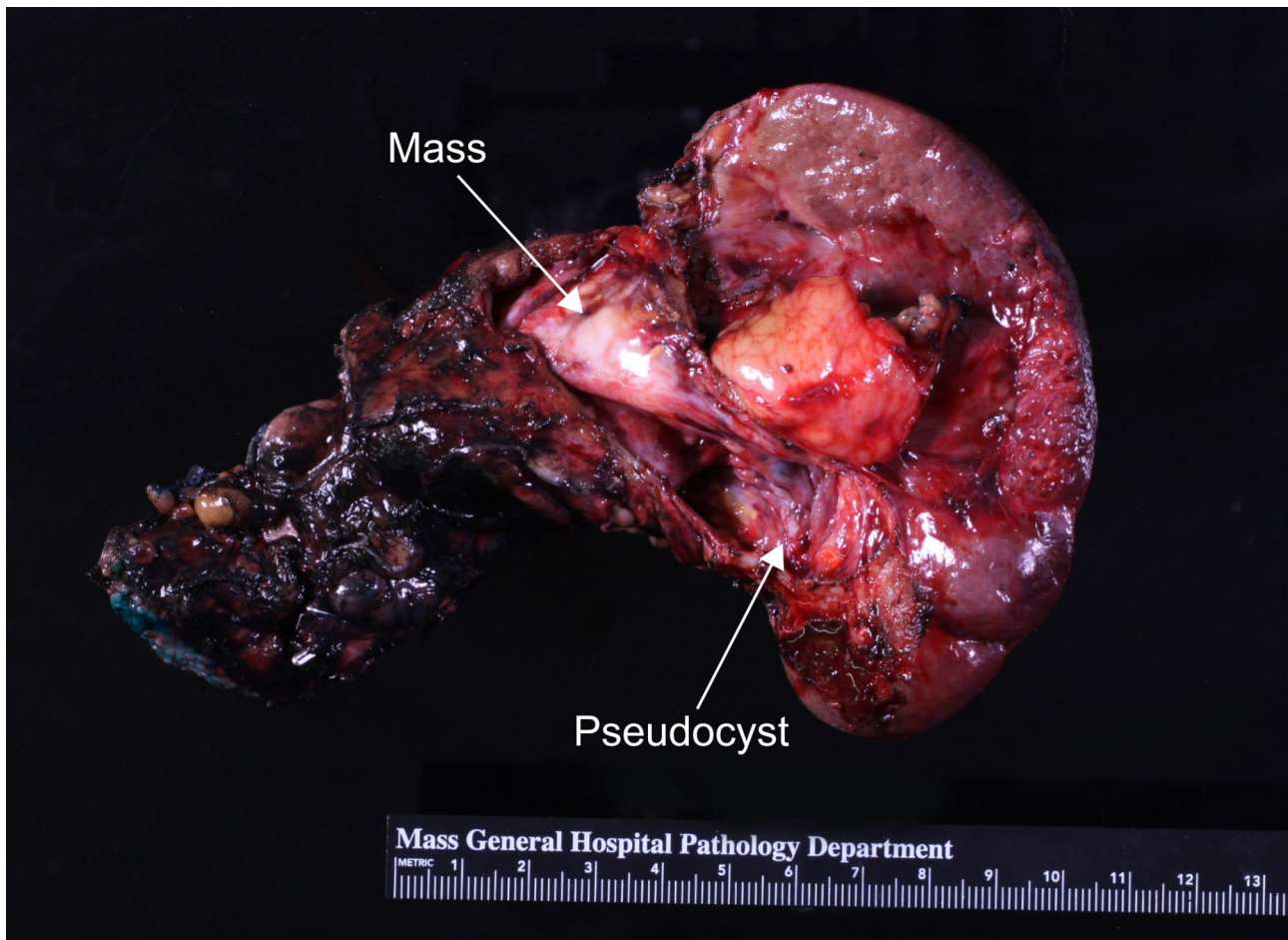
Fig. 3 Gross photograph of the distal pancreatectomy resection specimen showing a pancreatic body mass and tail pseudocyst encroaching the splenic hilum.

Challenges with making a distinction between G3 PanNET and PanNEC purely on morphologic grounds (not to mention inevitable interobserver variability) has led to the routine use of ancillary studies to support a diagnosis of one versus the other. Firstly, PanNECs generally have markedly elevated Ki67 proliferation indices>50% (as high as >90% in many small cell carcinomas), though a strict cutoff is not established for making this distinction [7–9]. Recently, Umetsu et al. reported an integrated approach for distinguishing G3 PanNETs from PanNECs using a panel of immunohistochemical markers as surrogates for genomic alterations: ATRX, P53, RB, and P16 [5]. In their cohort, loss of ATRX was entirely specific for G3 PanNET, though it was only seen in 18% of cases. Both *TP53* mutations and mutant P53 immunohistochemistry were seen in both groups. Loss of nuclear RB (41%) and diffuse P16 (65%) expression were entirely specific for PanNEC, though *CDKN2A* mutations were frequently seen in both groups (mutually exclusive with *TP53* mutations in G3 PanNET but frequently co-altered with *TP53* in PanNEC).

Despite these well-established findings, our case still did not neatly fit into one of the categories. Features supporting G3 PanNET included: the lower-grade liver metastasis, intermixed well-differentiated and higher-grade morphologies and only modestly elevated Ki67 index (20–30%). Features supporting PanNEC included: higher-grade morphologies that appeared to be compatible with carcinoma and exceed "well-differentiated" neuroendocrine morphology, retained ATRX and DAXX expression, and loss of RB expression. In addition, the finding of RB loss in the primary pancreatic tumor and retained RB expression in the liver metastasis is very unusual. One possibility is that there was a lower grade well-differentiated component of the primary neuroendocrine tumor with wildtype RB that metastasized, and now the primary neoplasm is predominated by a higher-grade component that later lost RB expression.

Interestingly, this patient was treated with everolimus, an inhibitor of mammalian target of rapamycin (mTOR), which was recently shown to provide a survival benefit in patients with metastatic well-differentiated PanNETs
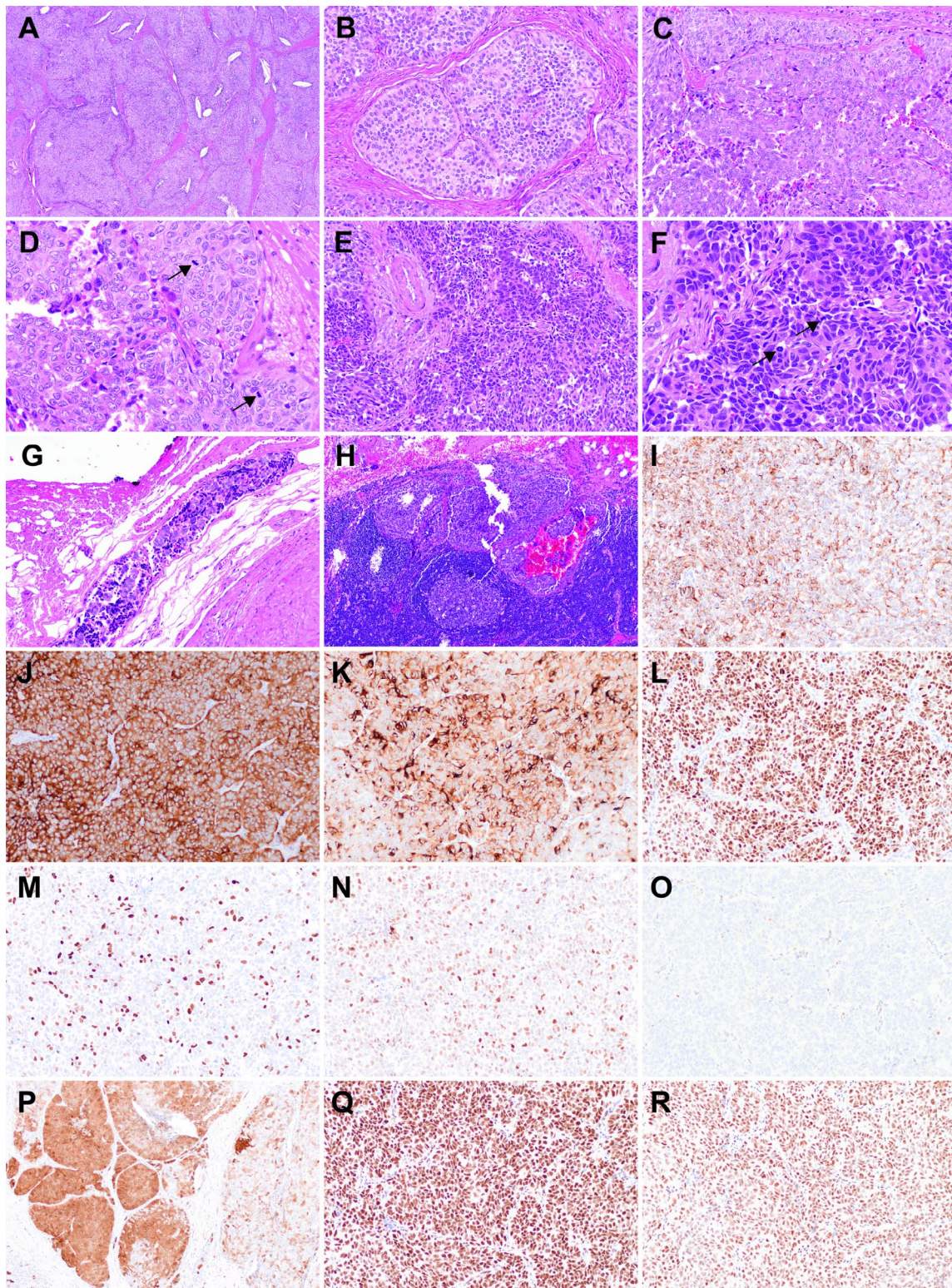
Fig. 4 Histology of pancreatic resection specimen. **(A)** Low-power nested appearance of the tumor (H&E, 40X). **(B)** Nest of well-differentiated appearing neuroendocrine tumor cells (H&E, 200X). **(C)** Area of higher-grade cells with enlarged irregular nuclei, vesicular chromatin, and **(D)** frequent mitoses (arrows) (H&E, 200X and 400X, respectively). **(E)** Area of higher-grade cells with irregular nuclei, dark smudgy chromatin, more scant cytoplasm, and **(F)** frequent mitoses (arrows) (H&E, 200X and 400X, respectively). **(G)** Lymphovascular invasion (H&E, 200X). (H) Metastasis to lymph node (H&E, 200X). Immunohistochemistry for MNF116 **(I)**, synaptophysin **(J)**, chromogranin **(K)**, INSM1 **(L)**, Ki67 **(M)**, P53 **(N)**, RB **(O)**, P16 **(P)**, ATRX **(Q)**, and DAXX **(R)**, all at 200X except P16 (100X).
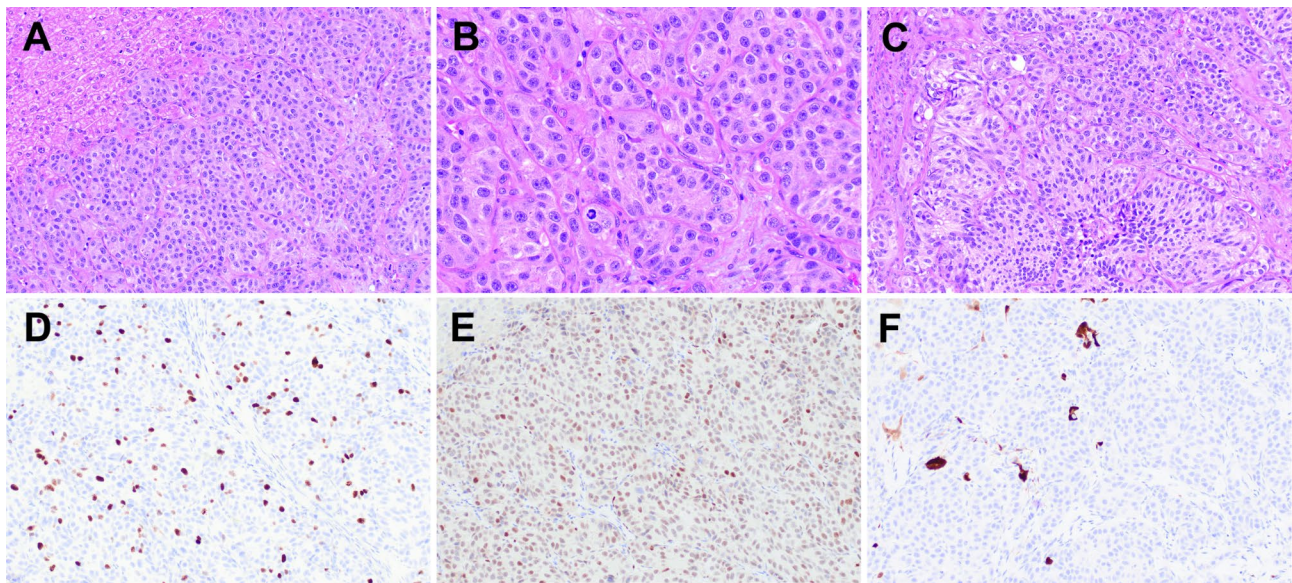
Fig. 5 Histology of liver resection specimen. **(A-C)** The tumor shows a nested appearance with monomorphic round-to-focally spindled nuclei with coarse granular chromatin and some prominent nucleoli. Occasional mitoses are seen (H&E, 200X, 400X, 200X, respectively). Immunohistochemistry for Ki67 in the hotspot region **(D)**, RB **(E)**, and P16 **(F)**, all at 200X.

[10]. Few studies have reported on the effects of everolimus on histopathologic examination, but one study found that everolimus downregulates the expression of Ki67 [11], which may be diagnostically relevant when interpreting Ki67 in treated specimens. We have not had extensive experience with evaluating histological specimens from post-everolimus treated PanNETs in our clinical practice, as most PanNETs are localized and cured with resection. In addition, we are aware that in general, tumor biology/morphology may change after treatment (well-documented after chemotherapy/radiation), though we were unable to find any specific literature discussing post-everolimus morphological changes. For our patient's tumor, the morphologies and Ki67 indices were similar between the pre-treatment biopsies and post-treatment resection specimens.

NGS was performed to further characterize the tumor but did not reveal any characteristic mutations (including lack of an *Rb* mutation, though other forms of *Rb* alterations such as loss of heterozygosity were not interrogated). *SMARCA4* loss of function has been described in a small subset of TTF1-negative neuroendocrine carcinomas of various sites [12], though no specific studies have investigated pancreatic neoplasms. Of the remaining identified mutations, *IRS2* amplification has been described in a small percentage (3%) of large cell neuroendocrine carcinomas of the lung [13] as well as a small percentage (15%) of small cell neuroendocrine carcinomas of the cervix [14].

In summary, we present a case highlighting some of the continued challenges that are faced when evaluating high-grade PanNENs. In addition, it raises the possibility that perhaps G3 PanNETs and PanNECs are not always entirely distinct and may lie on a spectrum or share some biological overlap in rare cases. While one explanation for the findings in this case is a collision of two distinct neoplastic processes, transformation from a well-differentiated PanNET (with retained RB expression, as seen in the liver metastasis) to a poorly differentiated PanNEC (with loss of RB expression), particularly given the admixture of varying morphologies—or something in between with intermediate prognosis—are of consideration.

Abbreviations

PanNEN	pancreatic neuroendocrine neoplasm
PanNET	well-differentiated pancreatic neuroendocrine tumor
PanNEC	poorly differentiated pancreatic neuroendocrine carcinoma
WHO	World Health Organization
G3	grade 3
CT	computed tomography
MRI	magnetic resonance imaging
EUS-FNAB	endoscopic ultrasound-guided fine needle aspiration biopsy
NGS	next-generation sequencing
VAF	variant allele frequency

Declarations

Ethics approval and consent to participate
The study was approved by the Dana Farber Cancer Institute (DFCI) Institutional Review Board (Protocol 02-240). The patient provided written consent for the participating in research activities.

Consent for publication
The patient provided written consent for the publication of this case report.

Competing interests
The authors declare no competing interests.

References

1. Who Classification of Tumours Editorial Board. Digestive System Tumours. International Agency for Research on Cancer; 2019.
2. Baughman AW, Wei NJ, Hahn PF, Casey BW, Zhang ML. Case 23-2022: a 49-Year-old man with hypoglycemia. N Engl J Med. 2022;387(4):356–65.
3. Ursprung S, Zhang ML, Asmundo L, Hesami M, Najmi Z, Cañamaque LG et al. An Illustrated Review of the Recent 2019 World Health Organization Classification of Neuroendocrine Neoplasms: A Radiologic and Pathologic Correlation. J Comput Assist Tomogr [Internet]. 2024; https://doi.org/10.1097/RCT.0000000000001593
4. Tang LH. Pancreatic Neuroendocrine Neoplasms: Landscape and Horizon. Arch Pathol Lab Med [Internet]. 2020; https://doi.org/10.5858/arpa.2019-0654-RA
5. Umetsu SE, Kakar S, Basturk O, Kim GE, Chatterjee D, Wen KW, et al. Integrated genomic and clinicopathologic Approach distinguishes pancreatic Grade 3 neuroendocrine Tumor from Neuroendocrine Carcinoma and identifies a Subset with Molecular Overlap. Mod Pathol. 2023;36(3):100065.
6. Tang LH, Untch BR, Reidy DL, O'Reilly E, Dhall D, Jih L, et al. Well-differentiated neuroendocrine tumors with a morphologically apparent high-Grade Component: a pathway distinct from poorly differentiated neuroendocrine carcinomas. Clin Cancer Res. 2016;22(4):1011–7.
7. Basturk O, Yang Z, Tang LH, Hruban RH, Adsay NV, McCall CM, et al. The high grade (WHO G3) pancreatic neuroendocrine tumor category is morphologically and biologically heterogeneous and includes both well differentiated and poorly differentiated neoplasms. Am J Surg Pathol. 2015;39(5):683.
8. Tang LH, Basturk O, Sue JJ, Klimstra DS. A practical Approach to the classification of WHO Grade 3 (G3) well-differentiated neuroendocrine tumor (WD-NET) and poorly differentiated neuroendocrine carcinoma (PD-NEC) of the pancreas. Am J Surg Pathol. 2016;40(9):1192–202.
9. Sorbye H, Welin S, Langer SW, Vestermark LW, Holt N, Osterlund P, et al. Predictive and prognostic factors for treatment and survival in 305 patients with advanced gastrointestinal neuroendocrine carcinoma (WHO G3): the NORDIC NEC study. Ann Oncol. 2013;24(1):152–60.
10. Smith D, Lepage C, Vicaut E, Dominguez S, Coriat R, Dubreuil O, et al. Observational study in a Real-World setting of targeted therapy in the systemic treatment of Progressive Unresectable or Metastatic Well-differentiated pancreatic neuroendocrine tumors (pNETs) in France: OPALINE Study. Adv Ther. 2022;39(6):2731–48.
11. Zhang HY, Cheng XB, Li Y, Jin LD, Yin HP. Effect of everolimus on the expression of Ki-67 and caspase-3 in patients with neuroendocrine tumors. Genet Mol Res [Internet]. 2017;16(1). https://doi.org/10.4238/gmr16019486
12. Gandhi JS, Alnoor F, Sadiq Q, Solares J, Gradowski JF. SMARCA4 (BRG1) and SMARCB1 (INI1) expression in TTF-1 negative neuroendocrine carcinomas including merkel cell carcinoma. Pathol Res Pract. 2021;219:153341.
13. George J, Walter V, Peifer M, Alexandrov LB, Seidel D, Leenders F, et al. Integrative genomic profiling of large-cell neuroendocrine carcinomas reveals distinct subtypes of high-grade neuroendocrine lung tumors. Nat Commun. 2018;9(1):1048.
14. Pei X, Xiang L, Chen W, Jiang W, Yin L, Shen X, et al. The next generation sequencing of cancer-related genes in small cell neuroendocrine carcinoma of the cervix. Gynecol Oncol. 2021;161(3):779–86.

Publisher's note
Springer Nature remains neutral with regard to jurisdictional claims in published maps and institutional affiliations.